Structure−Function Relationships of Human Liver Cytochromes P450 3A: Aflatoxin B1 Metabolism as a Probe[†]

Huifen Wang,[‡] Ryan Dick,[‡] Hequn Yin,[‡,§] Estefania Licad-Coles,[‡] Deanna L. Kroetz,[∥] Grazyna Szklarz,[⊥] Greg Harlow,[⊥] James R. Halpert,[⊥] and Maria Almira Correia*[,‡,∥]

Department of Cellular and Molecular Pharmacology, Department of Biopharmaceutical Sciences and Pharmaceutical Chemistry, and Liver Center, University of California, San Francisco, California 94143, and Department of Pharmacology and Toxicology, University of Arizona, Tucson, Arizona 85721

Received April 20, 1998; Revised Manuscript Received July 7, 1998

ABSTRACT: Cytochromes P450 3A4 and 3A5, the dominant drug-metabolizing enzymes in the human liver, share >85% primary amino acid sequence identity yet exhibit different regioselectivity toward aflatoxin B1 (AFB1) biotransformation [Gillam et al., (1995) *Arch. Biochem. Biophys. 317,* 374−384]. P450 3A4 apparently prefers AFB1 3α-hydroxylation, which results in detoxification and subsequent elimination of the hepatotoxin, over AFB1 *exo*-8,9-oxidation. In contrast, P450 3A5 is incapable of appreciable AFB1 3α-hydroxylation and converts it predominantly to the *exo*-8,9-oxide which is genotoxic. To elucidate the structural features that govern the regioselectivity of the human liver 3A enzymes in AFB1 metabolism and bioactivation, a combination of approaches including sequence alignment, homology modeling, and site-directed mutagenesis was employed. Specifically, the switch in AFB1 regioselectivity was examined after individual substitution of the divergent amino acids in each of the six putative substrate recognition sites (SRSs) of P450 3A4 with the corresponding amino acid of P450 3A5. Of the P450 3A4 mutants examined, P107S, F108L, N206S, L210F, V376T, S478D, and L479T mutations resulted in a significant switch of P450 3A4 regioselectivity toward that of P450 3A5. The results confirmed the importance of some of these residues in substrate contact in the active site, with residue N206 (SRS-2) being critical for AFB1 detoxification via 3α-hydroxylation. Moreover, the P450 3A4 mutant N206S most closely mimicked P450 3A5, not only in its regioselectivity of AFB1 metabolism but also in its overall functional capacity. Furthermore, the other SRS-2 mutant, L210F, also resembled P450 3A5 in its overall AFB1 metabolism and regioselectivity. These findings reveal that a single P450 3A5 SRS domain (SRS-2) is capable of conferring the P450 3A5 phenotype on P450 3A4. In addition, some of these P450 3A4 mutations that affected AFB1 regioselectivity had little influence on testosterone 6β-hydroxylation, thereby confirming that each substrate−P450 active site fit is indeed unique.

Cytochromes P450 (CYPs, P450s) 3A4 and/or 3A5 represent the major components of the human liver microsomal P450 complement and are involved in the metabolism of over 60% of clinically relevant drugs (*1*, *2*). These enzymes are also responsible for the activation and detoxification of hepatotoxic carcinogens such as aflatoxin B1 (AFB1)[1] (*3*−*5*). While P450 3A4 is the major isoform in the adult liver, P450 3A5 has been proposed to be polymorphically expressed. P450 3A5 is detected in approximately 25−30% of the adult livers examined, in which it represented 6−100% of the entire hepatic 3A content (*6*, *7*). P450 3A5 expression is apparently neither sex-specific nor unlike that of P450 3A4, drug-inducible, but may be age-related with significantly greater expression in adolescents (*6*, *7*). Although the protein sequences of P450s 3A4 and 3A5 are highly similar (*8*), human liver microsomal P450 3A5 as well as vaccinia virus-expressed P450 3A5 are catalytically inferior to the corresponding P450 3A4 preparations in their ability to metabolize certain drugs (*7*−*10*). Drugs such as nifedipine, testosterone, and cortisol are metabolized at a fraction of the P450 3A4 rates, while 17α-ethinylestradiol, quinidine, and erythromycin are very poorly or not at all metabolized (*7*−*10*). Although clearly, in the human liver microsomal membranes, P450 3A5 is functionally much less

[†] This research project was supported by NIDDKD grant DK26506 (MAC), NHLBI grant HL53994 (DLK) and NIGMS grant GM54995 (JRH) and a NIEHS Core Center Grant ES06694 (University of Arizona), from the National Institutes of Health. The authors also wish to acknowledge the UCSF Liver Center Core Spectrophotometry Component (supported by NIDDKD 26743).

* Correspondence to: Dr. M. A. Correia, Department of Cellular and Molecular Pharmacology, Box 0450, University of California, San Francisco, CA 94143-0450. Tel: 415-476-3992. Fax: 415-476-5292. E-mail: mariac@itsa.ucsf.edu.

[‡] Department of Cellular and Molecular Pharmacology, University of California.

[§] Present address: Department of Drug Metabolism & Pharmacokinetics, Hoffman-La Roche Inc., Nutley, NJ 07110.

[∥] Department of Biopharmaceutical Sciences and Pharmaceutical Chemistry, University of California.

[⊥] University of Arizona.-

[1] Abbreviations: AFB1, aflatoxin B1; AFM1, the 9a-hydroxylated AFB1; AFQ1, 3α-hydroxy AFB1; ALA, δ-aminolevulinic acid; b_5, cytochrome b_5; CHAPS, 3-[(3-cholamidopropyl)dimethylammonio]-1-propanesulfonate; DETAPAC, diethylenetriaminepentaacetic acid; EDTA, ethylenediaminetetraacetic acid; HPLC, high-pressure liquid chromatography; IPTG, isopropyl β-D-thiogalactopyranoside; PCR, polymerase chain reaction.

S0006-2960(98)00895-2 CCC: $15.00
Published on Web 08/21/1998

Scheme 1: P450-Dependent AFB1 Metabolism

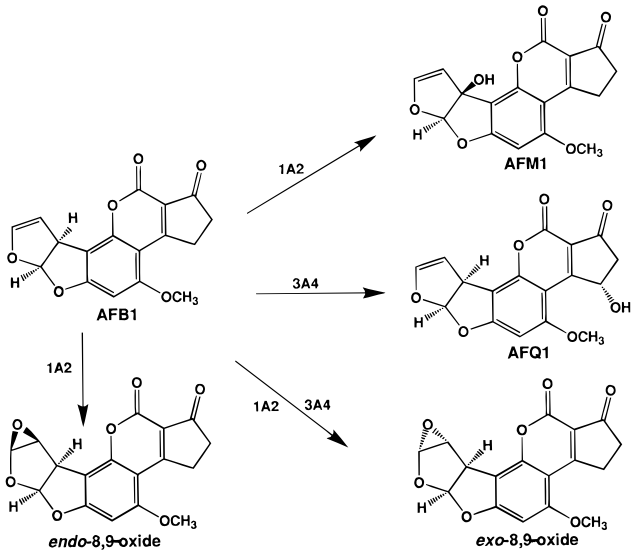

active than P450 3A4, the P450 3A5 enzyme purified from *Escherichia coli*-expressed cell membranes may be driven into a higher catalytic gear by manipulating the conditions for its functional reconstitution (*10*). It is to be underscored, however, that although such specialized conditions shed some light on the catalytic potential of the enzyme, they are not physiologically relevant. Physiologically, the inherent structure−function differences between the two enzymes (P450 3A4 vs P450 3A5) would prevail. However, even under these specialized reconstitution conditions, *P450 3A5 was incapable of appreciably detoxifying AFB1 via its 3α-hydroxylation and largely produced the genotoxic exo-8,9-epoxide* (Scheme 1) (*10*). It is conceivable that this failure of P450 3A5 may enhance the genotoxicity of AFB1 in individuals with near-exclusive P450 3A5 content.

Although P450s 3A4 and 3A5 are 84% identical in their primary sequence (*8*), their functional differences indicate that key differences in their active sites must exist. Unfortunately, no X-ray crystal structures for the mammalian P450s are available, but P450 homology models based on the crystallographic structures of P450s 101 (cam), 102 (BM-3), 107A1 (eryF), and 108 (terp), coupled with alignment based on comparative analyses of amino acid and coding sequences, hydropathy profiles, and secondary structure predictions (*11*−*18*), have identified putative substrate recognition sites (SRS) for P450s of the 1 and 2 families. Sequence inspection of closely related P450 isoforms, such as 2B1 and 2B2, 2A4, and 2A5, 2C3, and 2C4, reveals the critical importance of SRSs (*15*−*24*). Key differences could be singled out in select amino acid residues in certain SRS regions that confer functional competence and/or divergence, novel catalytic specificities and/or activities as well as specific regio- and stereoselective targeting of a given substrate (*18*), and the susceptibility of each structural mutant to mechanism-based inactivators [chloramphenicol and its analogues, secobarbital, ethynylnaphthalene, or aminobenzotriazole and its analogues (*23*−*27*)]. Such structure−function relationships suggest that specific SRS alterations can profoundly influence active site events. However, for a given mutant, the findings markedly differed with each substrate employed, underscoring the relative importance of each individual substrate−active site fit (*23*, *25*).

Detailed SRS analyses of P450s of the 3A family are just becoming available (*28*−*30*); 3A sequences have been aligned with those of P450s 101, 102, 107A1, and/or 108 (*12*, *17*, *18*), and homology-based P450 3A4 models have also been constructed (*31*−*33*). These analyses have revealed that *the 3A family, in common with other mammalian P450s, conforms to the overall topology of the bacterial P450 structures*. Although, in common with other P450s, SRS-4 and SRS-5 of P450s 3A are the only domains whose amino acid sequences can be aligned rather unambiguously with those of prokaryotic P450s (*17*, *18*), other residues in SRS-1 and SRS-3 regions, corresponding to helix B′, B′−C loop, and helix G, respectively, might play a role in substrate binding. Furthermore, although the closely related P450s 3A4 and 3A5 differ in 78 out of 503 amino acids, 17 of these variations fall within the 6 putative SRS domains (Chart 1). Any or all of these active site differences could influence the substrate binding and thereby account for the divergent catalytic behavior of P450 3A5 with a given substrate. These considerations, coupled with our knowledge that allelic variants and site-directed mutants of P450s with different catalytic properties have been particularly useful in pinpointing individual amino acid residues of potential functional relevance, led us to examine whether individual differences in the SRSs of P450s 3A4 and 3A5 would similarly identify the key determinants of their regioselectivity in AFB1 metabolism.

EXPERIMENTAL PROCEDURES

Materials. Testosterone and its hydroxylated metabolites, AFB1, AFQ1, δ-aminolevulinic acid (ALA), NADPH, glutathione (reduced form), sodium cholate, catalase, CHAPS, lysozyme, DETAPAC, and purified rat liver glutathione *S*-transferase (GST) were purchased from Sigma (St. Louis, MO). L-α-dilauroylphosphatidylcholine, L-α-dioleyl-*sn*-glycerophosphatidylcholine, and phosphatidylserine were obtained from Doosan Serdary Research Laboratories (Englewood Cliffs, NJ). DNase and RNase were purchased from Boehringer-Mannheim (Indianapolis, IN). Cytochrome b_5 (b_5) and cytochrome P450 reductase were purified from male rat liver microsomes according to previously reported methods (*34*). The glutathione adduct of *exo*-8,9-oxide of AFB1 was enzymatically synthesized from the corresponding *exo*-8,9-oxide (a gift from Prof. R. Harris, Vanderbilt University), purified by HPLC, and characterized spectrally (*35*). All other reagents were of the highest commercial purity.

Design of Site-Directed Mutants of CYP3A. Primary amino acid sequence alignment was carried out according to Nelson et al. (*17*). The putative substrate recognition region was determined according to the alignment of P450 3A4/P450 3A5 with that of P450s 101, 102, 107A1, and 108 and several mammalian P450s whose substrate recognition regions were determined previously (*17*, *18*). The putative site-directed mutants selected were as follows: SRS-1, P107S, F108L, and I120L; SRS-2, N206S and L210F; SRS-3, I238V; SRS-4, V296A; SRS-5, I369V, M371I, and V376T; SRS-6, S478D, L479T, and G480Q.

Site-Directed Mutagenesis of P450 3A. cDNAs for P450s 3A4 and 3A5 engineered to code for deletions of the N-terminal residues 3−12 and substitution of residue Ser18

Chart 1: Substrate Recognition Sites (SRS) of P450s 3A4 and 3A5

SUBSTRATE-RECOGNITION SITES OF P450s 3A4 & 3A5

SRS-1

3A4	**101**	V F T N R R P F G P V G F M K S A I S I A E D
3A5		V F T N R R **S L** G P V G F M K S A I S **L** A E D

SRS-2

3A4	**204**	V E N T K K L L
3A5		V E **S** T K K **F** L

SRS-3

3A4	**238**	I C V F P R E
3A5		**V S L** F P **K D**

SRS-4

294	E L V A Q S I I F I F A G Y E T T S S
	E L **A** A Q S I I F I F A G Y E T T S S

SRS-5

3A4	**368**	P I A M R L E R V
3A5		P **V** A **I** R L E R **T**

SRS-6

476	K L S L G G L L Q P
	K L **D T Q** G L L Q P

Table 1: List of Oligonucleotides and Screening Restriction Enzymes for Each P450 3A4 Mutation

mutation	oligonucleotide primer[a]	restriction enzyme
P107S	5′-CAC AAA CCG GAG GTC GTT TGG TCC AGT GGG-3′ 5′-CCC ACT GGA CCA AAG GAC CTC CGG TTT GTG-3′	*Stu*I (−)[c]
F108L	5′-CAC AAA CCG GAG GCC GTT GGG TCC AGT G-3′ 5′-CAC TGG ACC CAA CGG CCT CCG GTT TGT G-3′	*Stu*I (−)
I120L	5′-GAA AAG TGC CAT CTC TTT GGC TGA GGA TGA AG-3′[*]	*Bst*XI (+)
N206S	5′-CAA GAC CCC TTT GTG GAA AGT ACC AAG AAG CTT TTA AG-3′ 5′-CTT AAA AGC TTC TTG GTA CTT TCC ACA AAG GGG TCT TG-3′	*Rsa*I (+)
L210F	5′-AAA GAATGGATC CAA AAA ATC AAA TCT TAA AAA CTT CTT GGT GTT-3′ 5′-TTT TTG GAT CCA TTC TTT CTC TCA ATA ACA GTC-3′	*Hin*dIII (−)
I238V	5′-CT TGA AGT ATT AAA CGT GTG TGT GTT TCC AAG-3′[b]	*Afl*III (+)
V296A	5′-GTC CGA TCT GGA GCT GGC GGC CCA ATC AAT TAT C-3′ 5′-GAT AAT TGA TTG GGC CGC CAG CTC CAG ATC GGA C-3′	*Sac*I (−)
M371I	5′-TCC CAA TTG CTA TTC GAC TTG AGA GGG TC-3′[b]	*Taq*I (+)
V376T	5′-GCT ATG AGA CTT GAG AGG ACC TGC AAA AAA GAT GTT GAG-3′ 5′-CTC AAC ATC TTT TTT GCA GGT CCT CTC AAG TCT CAT AGC-3′	*BspM*I (+)
S478D	5′-CTG AAA TTA GAC CTT GGA GGA CTT CTT CAA CC-3′ 5′-GGT TGA AGA AGT CCT CCA AGG TCT AAT TTC AG-3′	*Sty*I (+)
L479T	5′-CTG AAA TTA AGC ACA GGA GGA CTT CTT CAA CC-3′ 5′-GGT TGA AGA AGT CCT CCT GTG CTT AAT TTC AG-3′	*Hin*dIII (−)
G480Q	5′-CTG AAA TTA AGC TTA CAA GGC CTT CTT CAA CC-3′ 5′-GGT TGA AGA AGG CCT TGT AAG CTT AAT TTC AG-3′	*Stu*I (+)

[a] The underlined nucleotide(s) was/were altered to introduce the desired mutation. [b] Generated via classical oligonucleotide-directed mutagenesis (*36*). [c] + or − refers to gain or loss of indicated restriction site.

with Phe and incorporated into the pCW vector, were gifts from Dr. R. Estabrook (SW Medical School, Dallas, TX). The 3A4 cDNA was removed from the pCW vector and inserted into pBluescript KS+ for generation of some of the mutants. QuikChange site-directed mutagenesis kit (Stratagene, La Jolla, CA) was used for the generation of the following mutants: P107S, F108L, N206S, V296A, V376T, S478D, L479T, and G480Q. The oligonucleotide pairs for each mutant are listed in Table 1. Mutants I120L, I238V, and M371I were constructed by the classical oligonucleotide-directed mutagenesis methods using uracil-containing single-stranded DNA from a 3A4/pBluescript KS+ phagemid and the oligonucleotides listed in Table 1 (*36*). The mutated P450 3A4 cDNAs were subsequently transferred to the pCW expression vector using standard cloning techniques. Mutant I369V was constructed as described previously (*29*). The mutant L210F was constructed by site-directed mutagenesis using the Expand High Fidelity PCR system (Boehringer-Mannheim, Indianapolis, IN) and the plasmid template pSE3A4His (*30*). The corresponding oligonucleotide pairs are listed in Table 1. Standard PCR conditions were used to generate the mutated cDNA. All mutants were screened by restriction enzyme digestion and confirmed by DNA sequencing.

Expression of Wild-Type P450s 3A4 and 3A5 and of P450 3A4 Point Mutants. The wild-type and mutant P450s 3A4 were expressed in *E. coli* XL-1 blue cells, *E. coli* DH5αF′ cells, or *E. coli* Topp3 cells according to published methods (*9*, *10*). Typically, a single colony from 2YT-Agar plate containing 100 μg/mL carbenicillin was innoculated into 100 mL of LB media containing 100 μg/mL carbenicillin and incubated overnight at 37 °C with shaking at 250 rpm. The overnight culture was used to seed 1 L of TB broth containing 0.2% BactoPeptone, 80 μg/mL ampicillin, and

appropriate amount of trace elements (*9*, *34*, *37*) and incubated at 37 °C, with shaking at 250 rpm. The heme precursor ALA (75 mg/L) was added when $OD_{600\ nm}$ reached ~0.3. P450 expression was induced by IPTG (238 mg/L) when $OD_{600\ nm}$ reached 0.5, at which time the incubation temperature was lowered to 30 °C. Bacterial cells were harvested at 20−26 h after induction, except for the *E. coli* Topp3 cells expressing the I369V mutant which were harvested ≈72 h after induction.

CHAPS Solubilization of E. coli-Expressed P450s. Bacterial cell membranes were prepared and solubilized according to John et al. (*38*) with modifications (inclusion of protease inhibitors during solubilization) as described (*34*). The membrane pellets obtained from cell lysates were washed once by resuspension in 80 mL of Mops buffer (100 mM Mops, pH 7.4, 10% glycerol, 1 mM EDTA, and 0.2 mM dithiothreitol) and resedimented. After resuspension in 20 mL of Mops buffer, 0.5% CHAPS was added and the mixture stirred gently at 4 °C for 4 h. The mixture was clarified by centrifugation at 100000*g* at 4 °C for 30 min, the supernatant was obtained, and the P450 content was assayed by the method of Omura and Sato (*39*). The solubilized membrane fractions were aliquoted and kept at −80 °C until use.

Immunoblotting of E. coli-Expressed Wild-Type and P450 3A4 Mutants. The authenticity of the expressed P450s as 3A proteins was verified by Western immunoblotting of the solubilized *E. coli* membranes against polyclonal anti-P450 3A IgGs raised in rabbits.

Testosterone Metabolism by Solubilized Recombinant Enzymes. Testosterone hydroxylase activity of the solubilized P450 proteins was determined as described (*40*), after initial optimization of the assay conditions using the wild-type enzyme and different molar ratios of P450 reductase and/or cytochrome b_5. From these preliminary studies, the molar ratio of P450 3A4:reductase:b_5 of 1:4:2 was selected with regard to near-optimal activity as well as conservative use of reagents and was adopted in all subsequent assays of the P450 3A4*wt* or its structural mutants. Briefly the assay conditions were as follows. The reagents were added at 4 °C in the following order: lipid mix (L-α-dilauroylphosphatidylcholine:L-α-dioleyl-*sn*-glycerophosphatidylcholine:phosphatidylserine, 1:1:1, w/w; 10 μg), sodium cholate (100 μg), cytochrome b_5 (20 pmol), P450 reductase (40 pmol), P450 3A4 or mutant (10 pmol), and GSH (1.5 mmol). The above mix was reconstituted at room temperature for 10 min and then placed back in ice. The following reagents were then added in order: Hepes buffer (50 mM, pH 7.85), catalase (100 U), DETAPAC (1 mM), water (q.s. 0.5 mL), $MgCl_2$ (30 mM), and [^{14}C]testosterone (0.25 mM). The mixture was preincubated at 37 °C for 2 min, and NADPH (1 mM) was added to start the reaction. The reaction was terminated with 1 mL of CH_2Cl_2. The metabolites were extracted twice with 2 mL of CH_2Cl_2, dried down under N_2, and assayed by HPLC with radioquantitation as described previously (*40*).

AFB1 Metabolism by Recombinant Enzymes. Functional assay of AFB1 metabolism by native and mutant enzymes was conducted as described by Ueng et al. (*41*) with some modifications to improve the enzyme activity and stability. Lipid mix (L-α-dilauroylphosphatidylcholine:L-α-dioleyl-*sn*-glycerophosphatidylcholine:phosphatidylserine, 1:1:1, w/w) was sonicated in water at a stock concentration of 0.5 μg/μL and stored at −20 °C. The following components were added in strict order: lipid mix (20 μg/mL), sodium cholate (200 μg/mL), cytochrome b_5 (200 pmol), cytochrome P450 reductase (400 pmol), solubilized bacterial membrane P450s (100 pmol), and reduced glutathione (3 mM). The mixture was incubated at room temperature followed by the addition of water, Hepes buffer (50 mM, pH 7.85), catalase (200 units/mL), DETAPAC (1 mM), $MgCl_2$ (30 mM), AFB1 (50 μM in 5 μL of methanol), purified rat liver glutathione *S*-transferase (0.2 mg/mL), and NADPH (1 mM) in a final volume of 0.5 mL. Because higher concentrations of CHAPS are inhibitory, its final concentration in the incubations was limited to 0.2%. The reaction was initiated by the addition of NADPH and stopped by the addition of 25 μL of 1.47 M formic acid after incubation with shaking (200 rpm) for 20 min at 37 °C. After vortexing, the protein was pelleted by centrifugation, and the supernatant was filtered through a Nylon membrane filter (Rainin Nylon-66, 0.45-μm pore size) and analyzed by HPLC as reported by Ueng et al. (*41*). Metabolites were characterized by comparison to authentic synthetic standards and quantified by integration of peak areas. In preliminary studies, cochromatography of the P450 3A4-dependent AFB1 metabolites with authentic GSH-AFB1 *endo*- and *exo*-8,9-oxides revealed that the enzyme exclusively catalyzed AFB1 *exo*-8,9-oxide formation, thereby confirming the findings of Ueng et al. (*41*). The formation of AFB1 *exo*-8,9-oxide was assessed by the combined yields of the corresponding GSH adduct and the diol formed during the reaction.

Computer Modeling of CYP3A4. The molecular model of cytochrome P450 3A4 was constructed previously (*33*), and the crystal structure of AFB1 (*42*) was obtained from the Cambridge Structural Database. The structures were displayed on a Silicon Graphics workstation using InsightII software (MSI, San Diego, CA). Energy minimization and molecular dynamics simulations were carried out with the Discover program, version 2.97 (MSI), using the consistent valence force field. The parameters for heme and ferryl oxygen were as descibed by Paulsen and Ornstein (*43*, *44*).

Aflatoxin B1 was docked into the active site of the P450 3A4 model in a reactive binding orientation leading to either *exo*-8,9-epoxidation or 3α-hydroxylation. In the case of epoxidation, the distance between C_8 of AFB1 and ferryl oxygen was 3 Å to allow for van der Waals contacts between these atoms leading to the initial electron abstraction from the substrate and the subsequent 8,9-epoxide formation. For 3α-hydroxylation, the C_3−ferryl oxygen distance was 3.7 Å and the $H_{3\alpha}$ was directed toward the O atom ($H_{3\alpha}$ was 2.6 Å from ferryl oxygen) to promote hydrogen bonding which is then followed by hydrogen abstraction. In both cases, the enzyme−substrate interactions were optimized by minimization of the side chains of protein residues within 5 Å from the substrate. The steepest descent method and harmonic potential were used, with a nonbond cutoff of 10 Å, and the energy minimization was carried out to a maximum gradient of 1 kcal mol^{-1} $Å^{-1}$. The nonbond interaction energy, both electrostatic and van der Waals forces, between the substrate and the enzyme was evaluated with the Docking module of the InsightII package.

In addition to AFB1 bound in a reactive binding orientation, a second AFB1 molecule was docked into the active site of P450 3A4 using molecular dynamics. For these

simulations, the first AFB1 molecule was fixed, while the second molecule along with the protein side chains within 5 Å from it was allowed to move. Initially, the system was minimized with the steepest descent method and then subjected to 1-ps molecular dynamics simulations followed by energy minimization, as described previously (*29*, *33*). The interactions of the second AFB1 molecule with the protein were also evaluated.

RESULTS

Optimization of P450, P450 Reductase, and Cytochrome b_5 Ratios in the Reconstituted System. In preliminary studies, we examined the requirement for cytochrome b_5 (b_5) and the molar ratios of P450 3A4, P450 reductase, and b_5 for optimal testosterone 6β-hydroxylase activity (results not shown). The P450 and b_5 ratios were initially maintained at 1:1, and the reductase molar ratios varied from 2 to 15, yielding near-maximal activity (≈19.8 nmol of 6β-hydroxytestosterone/nmol of P450/min) between 3 and 5 mol equiv of reductase. Next, when the P450:reductase molar ratios were maintained at 1:4, and the b_5 molar equivalents were varied from 0 to 3, near-maximal activity (≈21.5 nmol of 6β-hydroxytestosterone/nmol of P450/min) was observed with 2 mol equiv of b_5. This ratio also afforded maximal conservation of the protein reagents and was adopted in all subsequent experiments. It appeared that with some P450 3A4 mutants studied, the b_5 and reductase were important in stabilizing the P450 chromophore in the reconstituted system and that the stability of the P450 3A4 enzymes in the reconstituted system was critically dependent on the strict adherence to the indicated order of addition of the various components.

Authenticity of the Expressed P450s as 3A Proteins. After P450 expression, *E. coli* membranes were prepared, solubilized, and routinely subjected to Western immunoblotting against rabbit polyclonal anti-P450 3A IgGs to confirm the relatedness of the expressed P450s to the P450 3A4 protein (results not shown). Additional confirmation was derived from their ability to regio- and stereoselectively hydroxylate the testosterone molecule at the 6β- and 2β-sites (see below).

Regioselectivity of Testosterone Hydroxylation by P450s 3A4 and 3A5 and 3A4 Mutants. The functional relatedness of the P450 3A4 mutants to its parent P450s 3A4 and 3A5 was verified by determining the relative hydroxylation of testosterone at the 6β- and 2β-positions (Table 2). Testosterone 6β-hydroxylation serves as a diagnostic functional probe for most P450s 3A. The near-comparable activities of P450 3A4 mutants L210F, I238V, I369V, M371I, V376T, S478D, L479T, and G480Q revealed that they compared favorably to the wild-type in their ability to hydroxylate testosterone at the 2β- and 6β-positions. The other P450 3A4 mutants (P107S, F108L, I120L, and V296A) examined exhibited testosterone 6β-hydroxylase activities at values intermediate between those of P450s 3A4 and 3A5, while their testosterone 2β-hydroxylase activities were more comparable to that of P450 3A5*wt* rather than that of P4503A4. Mutant N206S exhibited a drastically reduced testosterone 6β-hydroxylase activity, with nondetectable testosterone 2β-hydroxylase activity. Nevertheless, the ability of most of the P450 3A4 mutants to hydroxylate testosterone at the 2β- and 6β-positions indicated their fidelity to each of these 3A functions. Of the mutants examined, only M371I appeared to deviate from this typical 3A functional behavior by exhibiting the additional and somewhat unusual capability of appreciably hydroxylating testosterone to a metabolite that coeluted with the 16β-hydroxytestosterone standard.

Table 2: Regioselectivity of Testosterone Hydroxylation by P450s 3A4 and 3A5 and Their Structural Mutants[a]

SRS domains	P450s	testosterone (T) hydroxylation (nmol of OH-T formed/nmol of P450/min) 6β-OHT	2β-OHT	6β/2β-OHT
	3A4*wt*	26.8 ± 3.91	1.85 ± 0.06	14.5
SRS-1	P107S	9.57	0.99	9.67
	F108L	9.79	0.34	28.8
	I120L	14.9	0.78	19.2
SRS-2	N206S	1.48 ± 0.11	ND[b]	
	L210F	27.4	1.54	17.8
SRS-3	I238V	29.0	2.1	13.8
SRS-4	V296A	9.04	0.19	47.6
SRS-5	I369V	23.8	2.49	9.56
	M371I[c]	18.7	1.29	14.5
	V376T	38.7	3.01	12.9
SRS-6	S478D	28.6	1.73	16.6
	L479T	17.2	1.04	16.5
	G480Q	25.2	1.25	20.0
	3A5*wt*	4.55 ± 2.37	0.79 ± 0.22	5.76

[a] Values listed are mean ± SD of at least three individual determinations or the mean of two individual determinations. The variability between each of the duplicate values was ≤5%. [b] ND, nondetectable. [c] A hydroxylated testosterone metabolite that coeluted with authentic 16β-OHT was also generated at the rate of 0.87 ± 0.25 nmol of OH-T formed/nmol of P450/min.

Regioselectivity of AFB1 Metabolism by P450 3A4 and Its Mutants. Consistent with previous reports, P450 3A4 was found to oxidize AFB1 to yield the 3α-hydroxy (AFQ1) and *exo*-8,9-oxide metabolites, at a metabolic ratio of 2.55 for AFQ1/8,9-oxide formation, while P450 3A5, as shown previously (*10*, *45*), was found to predominantly favor *exo*-8,9-oxidation over 3α-hydroxylation, with a corresponding ratio of 0.33 (Table 3). The rates of AFB1 *exo*-8,9-oxidation and 3α-hydroxylation of P450 3A5 were also found to be relatively much lower (≈7.5% and 1%, respectively) than those of P450 3A4, confirming previous reports (*10*, *45*). A cursory inspection of the data (Table 3) revealed that the most pronounced effects were elicited by mutations in P450 3A4 SRSs 2, 4, 5, and 6. Accordingly, mutation of P450 3A4 SRS-2 residue Asn206 to the corresponding P450 3A5 Ser residue yielded a mutant that was notably deficient in catalyzing AFB1 3α-hydroxylation and somewhat sluggish in catalyzing AFB1 *exo*-8,9-oxidation resulting in an AFB1 regioselectivity profile that more closely resembled that of P450 3A5 than that of P450 3A4. Similarly, the mutation of P450 3A4 SRS-2 residue Leu210 to the P450 3A5 residue Phe yielded an enzyme with considerably reduced AFB1 3α-hydroxylase and *exo*-8,9-oxidase activities, with metabolic ratios that also approached those of P450 3A5*wt*. Only a minor effect on the AFB1 regioselectivity profile was observed with the P450 3A4 SRS-4 mutant V296A, given the comparable (≈70%) lowering of each metabolic pathway. On the other hand, the mutation of P450 3A4 SRS-5 residue Ile369 to the corresponding P450 3A5 residue Val not only lowered the AFB1 3α-hydroxylase activity by 75% but also inhibited the *exo*-8,9-oxidase activity by >92%, such that the resulting mutant exhibited an apparent metabolic ratio of 8.5 for AFQ1/8,9-oxide formation. In contrast, the P450

Table 3: Regioselectivity OF AFB1 Hydroxylation by P450s 3A4 and 3A5 and Their Structural Mutants[a]

SRS domains	P450s	AFB1 hydroxylation (nmol of AFB1 metabolite formed/nmol of P450/min)		
		AFQ1	8,9-epoxide	AFQ1/8,9-epoxide
	3A4*wt*	2.04 ± 0.32	0.80 ± 0.14	2.55
SRS-1	P107S	1.11	1.01	1.10
	F108L	0.97	0.74	1.31
	I120L	2.65	0.96	2.76
SRS-2	N206S	0.08	0.29	0.28
	L210F	0.15	0.33	0.45
SRS-3	I238V	1.67	0.89	1.88
SRS-4	V296A	0.51	0.27	1.89
SRS-5	I369V	0.51	0.06	8.50
	M371I	2.23	1.34	1.66
	V376T	0.42	0.35	1.20
SRS-6	S478D	0.14	0.15	0.96
	L479T	0.20	0.17	1.18
	G480Q	0.46	0.29	1.59
	3A5*wt*[b]	0.02	0.06	0.33

[a] AFQ1 is the 3α-hydroxylated AFB1 metabolite. 8,9-*exo*-Epoxides were assayed by the combined yield of their GSH adducts and the diol species. Values listed are the mean ± SD of at least four individual determinations or the mean of at least two individual determinations. The variability between each of the duplicate values was ≤5%. [b] Traces of AFM1 (9a-hydroxy AFB1) were detected.

3A4 SRS-5 mutant V376T showed a minor tendency toward the P450 3A5 AFB1 regioselectivity profile largely because of a ≈80% decrease in AFB1 3α-hydroxylation but only a 56% decrease in 8,9-epoxidation. The P450 3A4 SRS-5 mutant M371I, on the other hand, showed a negligible switch toward the P450 3A5 regioselectivity profile largely because of its relatively enhanced (167%) capacity for AFB1 8,9-epoxidation. As predicted from homology modeling and molecular docking exercises, the divergent residues in the P450 3A5 SRS-6 region also considerably influenced its function. Accordingly, P450 3A4 SRS-6 mutants S478D and L479T showed marked >90% decreases in AFB1 3α-hydroxylation and ≈80% decreases in *exo*-8,9-epoxidation, with a consequently altered AFB1 regioselectivity profile. Much lesser effects (≈78% and 64% decreases, respectively) on AFB1 3α-hydroxylation and *exo*-8,9-epoxidation were manifested by the P450 3A4 SRS-6 mutant G480Q, with consequently negligible alteration of the AFB1 regioselectivity profile (Table 3).

The P450 3A4 SRS-1 mutants P107S and F108L also exhibited some switch toward the P450 3A5 AFB1 regioselectivity profile, albeit not as marked as that of N206S and L210F mutants. Accordingly, P450 3A4 SRS-1 mutants P107S and F108L exhibited decreases of ≈45−50% in AFB1 3α-hydroxylation, with little altered 8,9-epoxidation, that accordingly affected the overall regioselectivity profile. However, P450 3A4 SRS-3 mutant I238V showed little decrease in AFB1 3α-hydroxylation and no decrease in *exo*-8,9-epoxidation, with a correspondingly negligible switch toward the P450 3A5 AFB1 regioselectivity profile. On the basis of these results with I238V mutant and our computer modeling studies, the other P450 3A4 SRS-3 mutants (C239S, V240L, R243K, and E245D) were predicted to have even lesser effects and were not tested.

Computer Modeling. To gain some insight into enzyme−substrate interactions during AFB1 metabolism, we docked this substrate into the active site of the P450 3A4 model. When AFB1 is docked in an orientation leading to either its *exo*-8,9-epoxidation or 3α-hydroxylation, only residues 120, 369, 478, 479, and 480 of the residues studied are found within 5 Å from the substrate molecule (see Figures 1 and 2). However, the active site of P450 3A4 is large enough to accommodate two AFB1 molecules, in agreement with the positive cooperativity observed experimentally (*45*, *46*). Therefore, a second AFB1 molecule was also placed in the active site of the model, as shown in Figures 1 and 2. Additional amino acid residues such as 206, 210, and 238, which are found within 5 Å from the second AFB1 molecule, can now interact with the substrate. Furthermore, molecular dynamics simulations (up to 3 ps) indicated that the second substrate molecule may move freely within the active site and is able to approach other active site residues, such as 296 or 376. On the basis of docking results, major effects of residue replacement at positions 206, 210, and 369 can be linked to the alteration in the size of the amino acid side chain: a decrease in the case of N206S and I369V and an increase in the case of L210F. Furthermore, Asn206 may form hydrogen bonds with the second AFB1 molecule (not shown), which may affect substrate oxidation. On the other hand, mutation of residues that can interact with AFB1 only transiently, such as 296 or 376, led to only minor alterations in activity.

DISCUSSION

The above findings clearly reveal that not only does the P450 active site structure critically influence the catalytic course of the P450 reactions but also that each individual substrate−active site fit is unique. Thus, the active site differences between P450s 3A4 and 3A5 appear to critically influence the regioselectivity of AFB1 oxidation to a much greater extent than that of testosterone oxidation. In particular, residues Asn206, Leu210, Val296, Ile369, Val376, Ser478, Leu479, and Gly480 in the putative SRS domains 2, 4, 5, and 6 of P450 3A4, respectively, appear to be essential for the enzyme's catalytic generation of the 3α-hydroxy AFB1 metabolite, AFQ1. The replacement of these residues with the corresponding residues of P450 3A5 led to the drastic reduction, if not virtual abolition, of AFB1 3α-hydroxylation (Table 3). These four P450 3A4 SRS regions are also important for the expression of the P450 3A4 *exo*-8,9-epoxidase activity, as mutations to the corresponding P450 3A5 residues reveal (Table 3). Furthermore, the mutations of P450 3A4 SRS-2 residues Asn206 and Leu210 to the corresponding P450 3A5 residues Ser and Phe are sufficient to endow each mutant with the P450 3A5 phenotype, with near-comparable AFB1-oxidizing activities and metabolic ratios, thereby revealing the critical influence of each residue as a determinant of this phenotype. Collectively, these findings reveal that the SRS domains 2, 4, 5, and 6 of P450 3A4 are critical for anchoring AFB1 in an orientation that favors oxidation of the substrate at opposite (extreme) ends of the molecule. However, these P450 3A4 structural criteria cannot be generalized to its metabolism of other substrates, since in contrast to their marked influence on AFB1 metabolism, P450 3A4 mutants L210F, I369V, V376T, S478D, L479T, and G480Q had little, if any, effect on testosterone 6β- or 2β-hydroxylation (Table 2).

It is well-recognized, however, that the active site of P450s 3A is sufficiently large to accommodate more than one substrate molecule at a time, as the α-naphthoflavone (α-

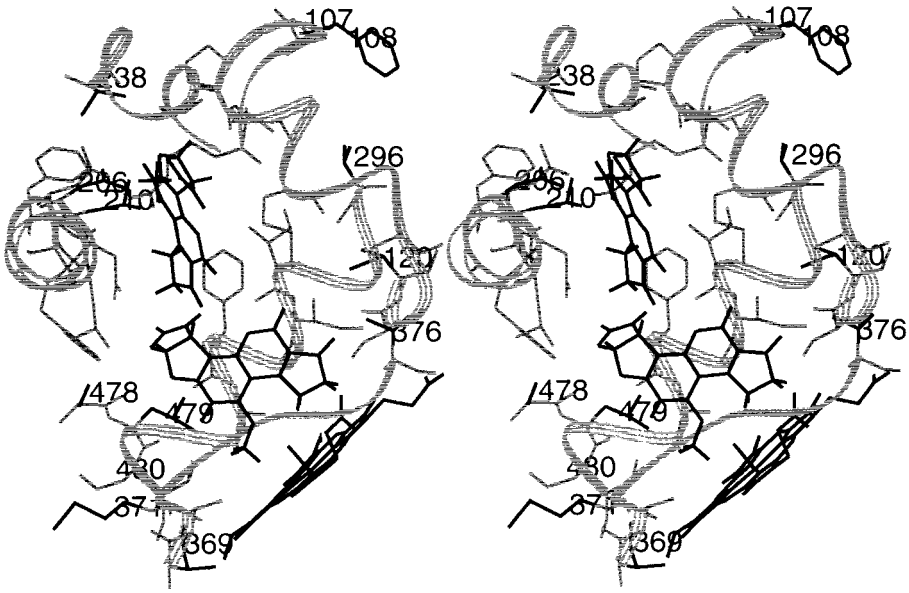

FIGURE 1: AFB1 docked into the active site of the P450 3A4 model in an orientation allowing for its 3α-hydroxylation, with the second substrate molecule also present in the active site. AFB1 molecules are displayed with all hydrogens and shown in black. The 3A4 residues studied are labeled and also shown in black, as is the heme moiety. Although the substrate molecule bound in a 3α-binding orientation (the molecule close to heme) can interact with only a limited number of protein residues, the second molecule may move close to other residues comprising the active site of P450 3A4.

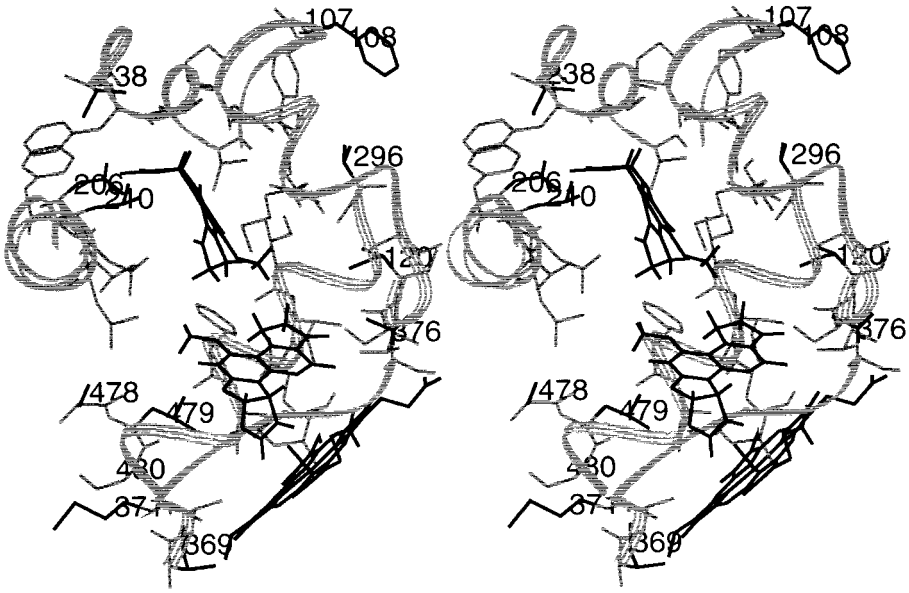

FIGURE 2: AFB1 docked into the active site of the P450 3A4 model in an orientation allowing for its *exo*-8,9-epoxidation, with the second substrate molecule also present in the active site. AFB1 molecules and heme are shown in black. The 3A4 residues studied are labeled and also shown in black. The AFB1 molecule bound in an orientation leading to its epoxidation (the molecule close to heme) can interact with a limited number of protein residues, but the second AFB1 molecule may be in contact with other active site residues.

NF) activation of P450 3A4-dependent metabolism of phenanthrene (*47*), AFB1 (*3*, *4*, *45*), and the steroids progesterone and testosterone (*28*) reveals. Furthermore, the catalytic behavior of P450 3A4 with regard to both AFB1 metabolic pathways, as revealed by typical sigmoidal v vs S kinetic plots, attests to positive cooperativity between AFB1 molecules within the P450 3A4 active site (*45*, *46*). Indeed, molecular docking studies confirm that the P450 3A4 active site is sufficiently large to accommodate two and even perhaps three AFB1 molecules, simultaneously. Thus, given such substrate packing, any spatial alteration of the active site cavity through mutation of individual active site residues that spatially interferes with this stacking could profoundly influence AFB1 metabolism, even though the residues altered are not in direct contact with the specific molecule targeted for metabolism.

Indeed such a "relay effect" may account for the loss of AFB1 3α-hydroxylation in the P450 3A4 N206S mutant. Docking of AFB1 in the P450 3A4 molecular model, coupled with energy minimization and molecular dynamics simulations, suggests that when AFB1 is docked in the 3α-binding orientation in the active site, a second AFB1 molecule can be docked in an orientation that would allow for hydrogen bond formation with Asn206 (not shown). The second molecule is then close enough to the first for van der Waals interactions, which would stabilize its 3α-binding orientation.

However, when AFB1 is bound in an orientation leading to *exo*-8,9-oxidation, the distance between the first molecule and the hydrogen-bonded second molecule is too large for direct interactions to occur. When Asn206 is replaced by Ser, the second AFB1 molecule can no longer form hydrogen bonds with Ser due to steric overlaps with other residues. This may lead to increased mobility of the second molecule, which would be unable to stabilize the 3α-binding orientation of the first. On the other hand, AFB1 epoxidation by the P450 3A4 N206S mutant would be affected to a lesser extent, in agreement with the experimental results. Similarly, when Leu210 is mutated to Phe, the steric bulk of this aromatic residue would interfere in the H-bonding of the Asn206 with the second AFB1 molecule, thereby accounting for the observed decrease in AFB1 3α-hydroxylation, with a lesser effect on AFB1 8,9-epoxidation. On the other hand, Ile369 is relatively close to the substrate bound in either a 3α-binding orientation or an orientation allowing for its epoxidation (Figures 1 and 2). Therefore, the substitution of Ile to Val at this position would directly influence either substrate binding orientation and account for the lowering of both AFB1 metabolic pathways. Such direct influence of the P450 3A4 I369V mutation on the target substrate is also observed with progesterone (*29*) *(*see below), but not with testosterone, since as in that report (*29*), we have found that there was little effect on testosterone 6*β*- or 2*β*-hydroxylation (Table 2).

The relatively reduced overall AFB1-oxidizing capacities of several individual P450 3A4 mutants that incorporated the corresponding residues of P450 3A5 suggest that several regions of the P450 3A5 active site structure must act in concert to significantly dampen the AFB1 metabolic capacity of P450 3A5*wt* relative to that of P450 3A4*wt*, with AFB1 *exo*-8,9-oxidation gaining relative prominence over the virtually abolished 3α-hydroxylation pathway. So how are the differences in the active site structures of these two enzymes manifested as differences in their function? It is unlikely that an unfavorable redox potential of the AFB1−P450 3A5 enzyme complex with consequent impairment of its reduction by P450 reductase is primarily responsible for its relatively inferior catalytic capacity, since the functional differential between the two enzymes persists even when this rate-limiting electron donation step is circumvented by surrogate O_2 donors, cumene hydroperoxide (CuOOH) and iodosobenzene (*45*). It is far more likely that this P450 3A5 functional deficit is due to a substrate−active site fit that allows considerably greater substrate mobility than that of P450 3A4. Indeed, the analysis of amino acid differences within the SRSs reveals that the majority of P450 3A4 residues in those regions are replaced with smaller amino acids in P450 3A5, which may increase the volume of the active site. Furthermore, two separate observations seem to support this view: (i) The detection of AFM1, the 9a-hydroxylated product, albeit in traces, after AFB1 incubation with the P450 3A5*wt* suggests that the P450 3A5 active site region that accommodates the AFB1 furan moiety might be somewhat more flexible (or less constrained) than that of P450 3A4, which fails to produce this metabolite in detectable amounts. (ii) The appreciable formation of 16*β*-hydroxytestosterone (or a metabolite that coelutes with it) by the P450 3A4 M371I mutant, in addition to 6*β*- and 2*β*-hydroxytestosterones, suggests that this P450 3A5 feature might allow far greater mobility of testosterone within its active site to enable oxidative attack at either end of the steroid molecule.

Furthermore, it appears that SRS regions other than 2, 4, 5, and 6 must participate in determining the overall functional potential of the P450 3A4 and P450 3A5 enzymes. For instance, Pro107 and Phe108 residues in the P450 3A4 SRS-1 domain, although seemingly protected from AFB1 by helix B′, exert some influence on AFB1 regioselectivity by lowering its 3α-hydroxylation to a considerably greater extent than its *exo*-8,9-oxidation, when the residues are mutated to the corresponding residues of P450 3A5. It is possible that residues Pro107 and especially Phe108 are part of the substrate access channel and thus influence AFB1−active site fit. Their localization in this domain may also account for their reduced activity with testosterone as the substrate (Table 2). The putative SRS-1 substrate-contacting Ile120 residue, on the other hand, exhibits little effect on either of the individual metabolic pathways or on AFB1 regioselectivity, when replaced with the corresponding P450 3A5 residue Leu120, given the conservative nature of this particular mutation. It is conceivable that the mutation of this residue to a less bulkier residue could affect AFB1 metabolism.

Mutation of the single divergent residue, Val296 in SRS-4 of P450 3A4 to the corresponding P450 3A5 residue Ala296, on the other hand, results in generally lowered activities of both AFB1 metabolic pathways. This residue is located at the N-terminal part of helix I and thus may affect the volume of the active site cavity and also may interact with the second AFB1 molecule. Substitution of Val296 with the P450 3A5 residue Ala would increase the volume of the active site and lead to increased mobility of AFB1, consistent with the observed lowering of both activities. Residue (M371) other than Ile369 in the P450 3A4 SRS-5 domain also appears to influence its AFB1 regioselectivity profile, as mutations to the corresponding residue of P450 3A5 reveal. The M371I mutant affects the regioselectivity profile by largely enhancing the *exo*-8,9-oxidation. This residue apparently comprises the substrate access channel and thus could influence the AFB1−active site fit.

The critical influence of this P450 3A4 SRS-5 region is underscored by the recent report that SRS-5 structural mutants profoundly affect its regioselectivity of progesterone hydroxylation and/or its testosterone 6*β*-hydroxylase activity (*29*). For instance, the P450 3A4 I369V mutant exhibited dramatically reduced progesterone 16α-hydroxylase activity, while the P450 3A4 A370V showed a marked increase in this activity. Apparently, residues 369 and 370 are found within 4 Å from the docked substrate and thus can interact through hydrophobic forces. Indeed mutation of Ile369 to Val decreases the van der Waals contacts with the substrate with consequently increased substrate mobility within the active site and loss of progesterone 16α-hydroxylase activity. Conversely, mutation of Ala370 to Val enhanced these interactions, which is reflected in considerably higher progesterone 16α-hydroxylase activity (*29*). The P450 3A4 L373H mutant, on the other hand, retained reactivity at the 6*β*- and 16α-progesterone sites as well as at the 6*β*-testosterone position but additionally produced a novel metabolite of each steroid (*29*). It is interesting in this regard, that in our hands, another P450 3A4 SRS-5 mutant M371I

also produced a novel testosterone metabolite that comigrated with 16β-hydroxytestosterone.

Collectively, these findings strongly support the notion that although key residues can be singled out as critical for a particular function, the global architecture of the individual active site participates in the intricate fine-tuning of the enzyme's catalytic interaction with any given substrate that ultimately defines its particular metabolic trajectory. This global P450 3A4 active site architecture apparently also dictates why the enzyme predominantly produces the genotoxic AFB1 *exo*-8,9-oxide instead of the equimixture of the *endo*- and *exo*-8,9-epoxides produced by human liver P450 1A2 (*41*). Molecular docking studies of AFB1 in the P450 3A4 active site reveal that the P450 3A4 active site structure cannot accommodate AFB1 in an orientation conducive for its *endo*-8,9-oxidation.

Although P450 3A5 appears to favor the AFB1 genotoxogenic metabolic pathway, the genotoxic potential of P450 3A5 is but a mere fraction of that of P450 3A4*wt*. As such, is the genotoxic potential of P450 3A5 of any clinical significance? As discussed earlier, given its overall negligible detoxification of AFB1, the P450 3A5 preference for the genotoxic *exo*-8,9-oxidation pathway would be of concern to individuals that predominantly express this hepatic isoform. While human liver P450 1A2 also metabolizes AFB1 to AFM1 (a major metabolite) and a mixture of *endo*- and *exo*-8,9-oxides, its relative role in AFB1 activation to the genotoxic *exo*-8,9-oxide apparently is secondary to that of P450 3A4, in a direct comparison of the two enzymes in metabolic as well as carcinogenic bioactivation assays, according to one report (*41*). However, this particular issue remains controversial (*41*, *46*) and may actually relate to the relative activity of each P450 isoform at a given (micromolar or submicromolar) AFB1 substrate concentration. Furthermore, although the P450 1A2-catalyzed AFM1 formation is a detoxification process, the overall extent of such detoxification is considerably inferior to that (AFQ1 formation) of P450 3A4 and secondary to its own potential for AFB1 *endo*- and *exo*-8,9-oxidation. Thus, the relative risk of hepatocarcinogenic AFB1 bioactivation would be enhanced in individuals that not only exhibit a high content of both P450 1A2 and P450 3A5 but are also chronically exposed to low-grade dietary AFB1, given (i) the overall relatively poor capacity for AFB1 detoxification expected in this population, (ii) the lack of human GST enzymes capable of detoxifying the *endo*- and *exo*-8,9-oxides, and (iii) the inability of human epoxide hydrolase to significantly enhance the detoxication of *endo*- and *exo*-8,9-oxides (*48*). Given this scenario, a retrospective analysis to determine whether the population infected with the hepatitis B virus that was also found to be at risk for AFB1 hepatocarcinogenesis in epidemiological studies is a population that predominantly exhibited the P450 3A5 phenotype would be of clinical interest.

ACKNOWLEDGMENT

The authors sincerely thank Prof. R. W. Estabrook (South Western Medical School, Dallas, TX) for the P450 3A4 and 3A5 plasmids, Prof. R. Harris (Vanderbilt University, Nashville, TN) for the gift of AFB1 *exo*-8,9-oxide, and Dr. You-Ai He (University of Arizona, Tucson, AZ) who provided the plasmid for the expression of the P450 3A4 mutant I369V. We also thank Dr. Kung Ming Covitz, Dept of Biopharmaceutical Sciences, UCSF, for her expert advice and helpful suggestions in the generation of the mutants by the Kunkel method.

REFERENCES

1. Wrighton, S. A., and Stevens, J. C. (1992) *Crit. Rev. Toxicol. 22*, 1−21.
2. Guengerich, F. P. (1995) in *Cytochrome P450: Structure, Mechanism and Biochemistry* (Ortiz de Montellano, P. R., Ed.) pp 473−574, Plenum Press, New York, NY.
3. Raney, K. D., Shimada, T., Kim, D. H., Groopman, J. D., Harris, T. M., and Guengerich, F. P. (1992) *Chem. Res. Toxicol. 5*, 202−210.
4. Ramsdell, H. S., Parkinson, A., Eddy, A. C., and Eaton, D. L. (1991) *Toxicol. Appl. Pharmacol. 108*, 436−447.
5. Gallagher, E. P., Wienkers, L. C., Stapleton, P. L., Kunze, K. L., and Eaton, D. L. (1994) *Cancer Res. 54*, 101−108.
6. Wrighton, S. A., Ring, B. J., Watkins, P. B., and Vanden-Branden, M. (1989) *Mol. Pharmacol. 36*, 97−105.
7. Wrighton, S. A., Brian, W. R., Sari, M.-A., Iwasaki, M., Guengerich, F. P., Raucy, J. L., Molowa, D. T., and Vandenbranden, M. (1990) *Mol. Pharmacol. 38*, 207−213.
8. Aoyama, T., Yamano, S., Waxman, D. J., Lapenson, D. P., Meyer, U. A., Fischer, V., Tyndale, R., Inaba, T., Kalow, W., Gelboin, H. V., and Gonzalez, F. J. (1989) *J. Biol. Chem. 264*, 10388−10395.
9. Gillam, E. M., Baba, T., Kim, B. R., Ohmori, S., and Guengerich, F. P. (1993) *Arch. Biochem. Biophys. 305*, 123−131.
10. Gillam, E. M., Guo, Z., Ueng, Y. F., Yamazaki, H., Cock, I., Reilly, P. E., Hooper, W. D., and Guengerich, F. P. (1995) *Arch. Biochem. Biophys. 317*, 374−384.
11. Poulos, T. L., Finzel, B. C., and Howard, A. J. (1987) *J. Mol. Biol. 195*, 687−700.
12. Nelson, D. R., and Strobel, H. W. (1988) *J. Biol. Chem. 263*, 6038−6050.
13. Gotoh, O. (1992) *J. Biol. Chem. 267*, 83−90.
14. Hasemann, C. A., Kurumbail, R. G., Boddupali, S. S., Peterson, J. A., and Deisenhofer, J. (1995) *Structure 3*, 41−62.
15. Johnson, E. F. (1992) *Trends Pharmacol. Sci. 13*, 122−126.
16. Korzekwa, K. R., and Jones, J. P. (1993) *Pharmacogenetics 3*, 1−18.
17. Nelson, D. R. (1995) In *Cytochrome P450: Structure, Function, and Mechanism* (Ortiz de Montellano, P. R., Ed.) 2nd ed., pp 575−606, Plenum Press, New York, NY.
18. von Wachenfeldt, C., and Johnson, E. F. (1995) In *Cytochrome P450: Structure, Mechanism and Biochemistry* (Ortiz de Montellano, P. R., Ed.) pp 183−223, Plenum Press, New York, NY.
19. Lindberg, R. L., and Negishi, M. (1989) *Nature 339*, 632−634.
20. Kronbach, T., and Johnson, E. F. (1991) *J. Biol. Chem. 266*, 6215−6220.
21. Hsu, M. H., Griffin, K. J., Wang, Y., Kemper, B., and Johnson, E. F. (1993) *J. Biol. Chem. 268*, 6939−6944.
22. He, Y. A., Balfour, C. A., Kedzie, K. M., and Halpert, J. R. (1992) *Biochemistry 31*, 9220−9226.
23. He, Y. Q., He, Y. A., and Halpert, J. R. (1995) *Chem. Res. Toxicol. 8*, 574−579.
24. Szklarz, G. D., He, Y. A., and Halpert, J. R. (1995) *Biochemistry 34*, 14312−14322.
25. He, K., He, Y. A., Szklarz, G., Halpert, J. R., and Correia, M. A. (1996) *J. Biol. Chem. 271*, 25864−25872.
26. Roberts, E. S., Pernecky, S. J., Alworth, W. L., and Hollenberg, P. F. (1996) *Arch. Biochem. Biophys. 331*, 170−176.
27. Kent, U. M., Hanna, I. H., Szklarz, A., Vaz, G. D., Halpert, J. R., Bend, J. R., and Hollenberg, P. F. (1997) *Biochemistry 36*, 11707−11716.
28. Harlow, G., and Halpert, J. R. (1997) *J. Biol. Chem. 272*, 53996−54002.

29. He, Y. A., He, Y. Q., Szklarz, G. D., and Halpert, J. R. (1997) *Biochemistry 36*, 8831−8839.
30. Domanski, T. L., Liu, J., Harlow, G. R., and Halpert, J. R. (1998) *Arch. Biochem. Biophys. 350*, 223−232.
31. Zvelebil, M. J. J. M. M., Wolf, C. R., and Sternberg, M. J. E. (1991) *Protein Eng. 4*, 271−282.
32. Lewis, D. F., Eddershaw, P. J., Goldfarb, P. S., and Tarbit, M. H. (1996) *Xenobiotica 26*, 1067−1086.
33. Szklarz, G. D., and Halpert, J. R. (1997) *J. Comput.-Aided Mol. Des. 11*, 265−272.
34. Licad-Coles, E., He, K., Yin, H., and Correia, M. A. (1997) *Arch. Biochem. Biophys. 338*, 35−42.
35. Raney, K. D., Meyer, D. J., Ketterer, B., Harris, T. M., and Guengerich, F. P. (1992) *Chem. Res. Toxicol. 5*, 470−478.
36. Kunkel, T. A., Roberts, J. D., and Zakour, R. A. (1987) *Methods Enzymol. 154*, 367−382.
37. Ren, S., Liu, H., Licad, E., and Correia, M. A. (1996) *Arch. Biochem. Biophys. 333*, 96−102.
38. John, G. H., Hasler, J. A., He, Y.-A., and Halpert, J. R. (1994) *Arch. Biochem. Biophys. 314*, 367−375.
39. Omura, T., and Sato, R. (1964) *J. Biol. Chem. 239*, 2370−2378.
40. Underwood, M. C., Cashman, J. R., and Correia, M. A. (1992) *Chem Res. Toxicol. 5*, 42−53.
41. Ueng, Y. F., Shimada, T., Yamazaki, H., and Guengerich, F. P. (1995) *Chem. Res. Toxicol. 8*, 218−225.
42. van Soest, T. C. (1970) *Acta Crystallogr., Sect. B 26*, 1947.
43. Paulsen, M. D., and Ornstein, R. L. (1991) *Proteins 11*, 184−204.
44. Paulsen, M. D., and Ornstein, R. L. (1992) *J. Comput.-Aided Mol. Des. 6*, 449−460.
45. Ueng, Y. F., Kuwabara, T., Chun, Y.-J., and Guengerich, F. P. (1997) *Biochemistry 36*, 370−381.
46. Gallagher, E. P., Kunze, K. L., Stapleton, P. L., and Eaton, D. L. (1996) *Toxicol. Appl. Pharmacol. 141*, 595−606.
47. Shou, M., Grogan, J., Mancewicz, J. A., Krausz, K. W., Gonzalez, F. J., Gelboin, H. V., and Korzekwa, K. R. (1994) *Biochemistry 33*, 6450−6455.
48. Johnson, W. W., Yamazaki, H., Shimada, T., Ueng, Y. F., and Guengerich, F. P. (1997) *Chem. Res. Toxicol. 10*, 672−676.

BI980895G